The EMBO Journal (2009) 28, 2554–2567 | © 2009 European Molecular Biology Organization | Some Rights Reserved 0261-4189/09
www.embojournal.org

THE EMBO JOURNAL

EMBO open

FG/FxFG as well as GLFG repeats form a selective permeability barrier with self-healing properties

Steffen Frey and Dirk Görlich*

Max-Planck-Institut für Biophysikalische Chemie, Am Fassberg, Göttingen, Germany

The permeability barrier of nuclear pore complexes (NPCs) controls all nucleo-cytoplasmic exchange. It is freely permeable for small molecules. Objects larger than ≈30 kDa can efficiently cross this barrier only when bound to nuclear transport receptors (NTRs) that confer translocation-promoting properties. We had shown earlier that the permeability barrier can be reconstituted in the form of a saturated FG/FxFG repeat hydrogel. We now show that GLFG repeats, the other major FG repeat type, can also form highly selective hydrogels. While supporting massive, reversible importin-mediated cargo influx, FG/FxFG, GLFG or mixed hydrogels remained firm barriers towards inert objects that lacked nuclear transport signals. This indicates that FG hydrogels immediately reseal behind a translocating species and thus possess 'self-healing' properties. NTRs not only left the barrier intact, they even tightened it against passive influx, pointing to a role for NTRs in establishing and maintaining the permeability barrier of NPCs.

The EMBO Journal (2009) **28,** 2554–2567. doi:10.1038/emboj.2009.199; Published online 13 August 2009
Subject Categories: membranes & transport
Keywords: hydrogel; nucleoporin; nuclear pore complex; permeability barrier; selective phase model

Introduction

Nuclear pore complexes (NPCs) are giant molecular assemblies that control the exchange of macromolecules between the nucleus and the cytoplasm (Mattaj and Englmeier, 1998; Görlich and Kutay, 1999; Adam, 2001; Macara, 2001; Rout and Aitchison, 2001; Pemberton and Paschal, 2005; Tran and Wente, 2006; D'Angelo and Hetzer, 2008). They pose a firm passive diffusion barrier for inert molecules larger than ≈2.5 nm in radius (see Mohr *et al*, 2009), but at the same time, NPCs remain highly permeable for shuttling nuclear transport receptors (NTRs) and even very large NTR•cargo complexes (Newmeyer *et al*, 1986; Mohr *et al*, 2009). Examples for NTRs are the prototypical nuclear import receptor importin β (Impβ) (Chi *et al*, 1995; Görlich *et al*, 1995; Iovine *et al*, 1995) and exportin 1/CRM1 (Fornerod *et al*, 1997; Stade *et al*, 1997). Typically, a nuclear transport signal on a cargo molecule mediates its interaction with an NTR. The IBB domain, for example, allows direct binding to Impβ and constitutes one of the strongest known nuclear import signals (Weis *et al*, 1996; Görlich *et al*, 1996a).

Facilitated NPC passage is not directly coupled to ATP or GTP hydrolysis (Schwoebel *et al*, 1998; Englmeier *et al*, 1999; Ribbeck *et al*, 1999). Nevertheless, the nuclear transport machinery is able to pump cargoes against gradients of chemical activity. This is possible, because the RanGTPase system switches the shuttling NTRs in a compartment-specific manner between their low- and high-affinity forms for cargo binding (Rexach and Blobel, 1995; Görlich *et al*, 1996b; Fornerod *et al*, 1997; Kutay *et al*, 1997a).

NPCs are composed of multiple copies of ≈30 different proteins known as nucleoporins or Nups (Rout *et al*, 2000). Nups not only form the rigid NPC scaffold but many of them also contain non-globular, natively unfolded protein modules typically containing FG repeats (Hurt, 1988; Denning *et al*, 2003). FG repeat domains are essential for viability (Strawn *et al*, 2004) and comprise up to 50 repeat units. Each unit contains a hydrophobic cluster, typically of the sequence FG, FxFG or GLFG, which is embedded into a more hydrophilic spacer sequence (Denning and Rexach, 2007). FG repeats bind NTRs during facilitated NPC passage. Mutant NTRs that are defective in FG repeat binding also display defects in facilitated NPC passage (Iovine *et al*, 1995; Bayliss *et al*, 1999, 2000; Ribbeck and Görlich, 2001; Bednenko *et al*, 2003).

It is, however, a challenging task to explain how NPCs hinder the passive passage of inert material and how an NTR•FG repeat interaction promotes facilitated translocation. If the central channel of NPCs were lined with isolated binding sites for NTRs, then one would expect retention and delayed passage of the bound species. Such simple arrangement also gives no plausible explanation as to how inert material is selectively excluded from passage. The facts that any given NTR possesses multiple binding sites for FG repeats (Bayliss *et al*, 2002; Bednenko *et al*, 2003; Morrison *et al*, 2003; Isgro and Schulten, 2005) and, conversely, that FG repeat domains comprise multiple NTR-binding motifs indeed suggest that facilitated translocation involves more complicated interactions than only a binary binding between a receptor and isolated FG motifs.

To solve these problems, we previously proposed the selective phase or hydrogel model, which assumes that the central permeability barrier of NPCs consists of an FG repeat hydrogel (Ribbeck and Görlich, 2001, 2002). Indeed, it has been shown that the FG/FxFG repeat domain from the yeast Nup Nsp1p not only formed a hydrogel as predicted (Frey *et al*, 2006) but also displayed permeability properties very

*Corresponding author. Department of Cellular Logistics, Max-Planck-Institut für Biophysikalische Chemie, Am Fassberg 11, Göttingen 37077, Germany. Tel.: +551 201 2401; Fax: +551 201 2407;
E-mail: goerlich@mpibpc.mpg.de

Received: 12 January 2009; accepted: 18 June 2009; published online: 13 August 2009

similar to those of authentic NPCs and allowed an up to 20 000-fold faster entry of a large NTR•cargo complex compared with the cargo alone (Frey and Görlich, 2007). To achieve this exquisite selectivity, the concentration of the FG hydrogel has to exceed a saturation limit of about 100 mg/ml, a concentration that is most probably exceeded also within authentic NPCs (Frey and Görlich, 2007).

The formation of an FG hydrogel relies on multivalent interactions between FG repeat domains. An FG hydrogel can therefore be considered a three-dimensional meshwork and the exclusion of inert material can be explained by a sieving effect according to the size of the meshes.

NTR•cargo complexes are typically far larger than the passive NPC exclusion limit and the expected size of the meshes. Their passage through NPCs must therefore involve a transient opening of those meshes that would otherwise obstruct their path. The hydrophobic clusters of the FG repeats not only bind NTRs but they are also required for gel formation and hence also for creating inter-repeat contacts (Frey *et al*, 2006). Binding of an NTR to these hydrophobic clusters might therefore destabilise and transiently open adjacent meshes, thereby allowing the receptor to enter the barrier (Ribbeck and Görlich, 2001).

In this study, we show that not only FG/FxFG repeats but also GLFG repeats—the dominant repeat type of yeast NPCs—form highly selective hydrogels. GLFG gels suppressed the passive influx of inert material, but also allowed a more than three orders of magnitude faster entry of NTRs and their cargo complexes. This applied not only to yeast and mammalian importins but also to the exportin Crm1p. We also show that the entry of NTRs into an FG hydrogel is reversible and that RanGTP facilitates the exit of an Impβ•cargo complex from the gel. We observed that FG hydrogels suppressed the passive entry of inert material even when a massive influx of NTR•cargo complexes occurred, which mirrors the behaviour of authentic NPCs. This suggests that the resealing of the permeability barrier behind a translocating species does not require the complex composition and architecture of an NPC, but is instead mediated by the FG repeats themselves. Interestingly, NTRs even tightened the hydrogels against passive influx, pointing to a role for NTRs in establishing and maintaining the permeability barrier of nuclear pores. In the accompanying study (Mohr *et al*, 2009), we show that the dominant-negative human Impβ$^{45\text{-}462}$ fragment (hsImpβ$^{45\text{-}462}$) (Kutay *et al*, 1997b) not only blocks facilitated NPC passage but also lowers the passive exclusion limit. We show here that these two striking effects are also observed with a GLFG hydrogel: The inhibitor hindered not only gel entry but also the intra-gel movement of the diffusing species. Thus, *in vitro* assembled FG hydrogels, despite their simple composition, reproduced all aspects of NPC permeability tested so far. This strongly supports the model that the NPC permeability barrier indeed is an FG hydrogel.

Results

The barrier formed by an FG hydrogel reseals immediately behind a translocating species

We previously showed that a saturated FG hydrogel restricts the influx of inert material, but permits an up to 20 000-fold faster entry of Impβ•cargo complexes that were 5-fold larger in mass than the inert reference object (Frey and Görlich, 2007). To mediate their entry into the gel, importins must locally perforate the hydrogel. If such perforations remained open or persisted for too long in authentic NPCs, then the permeability barrier would break down and nuclear and cytoplasmic contents would intermix (Figure 1A and B). However, NPCs remain strict barriers towards inert objects even when large NTR•cargo complexes pass (Newmeyer *et al*, 1986; accompanying study). Perforations in that context must therefore be extremely short lived and reseal immediately behind any translocating species (Figure 1C). It was, however, unclear whether FG repeat domains and NTRs are sufficient for resealing and whether *in vitro* assembled FG hydrogels reproduce NPC properties authentically enough to stay sealed against inert material even when NTRs penetrate the gel.

To address these questions, we chose MBP-mCherry, a 70-kDa fusion between the maltose-binding protein (SwissProt P0AEY0) and the monomeric red fluorescent protein mCherry (Shaner *et al*, 2004) as an inert permeation probe, and the FG/FxFG repeat domain from Nsp1p (Hurt, 1988) as the building block of a saturated FG hydrogel. The influx of MBP-mCherry alone was slow, but still measurable (Figures 2C and 3A, Table I). We then pre-mixed 3 μM of

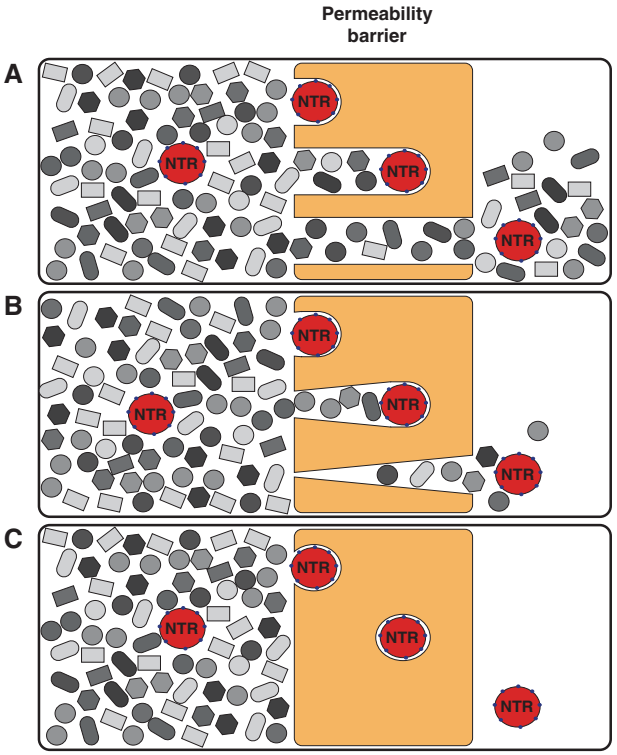

Figure 1 Resealing modes of the permeability barrier. Cartoons sketch conceivable behaviours of the barrier towards nuclear transport receptors (NTRs) and inert material. (**A**) A scenario in which NTRs can penetrate into and through the barrier, but where no resealing behind the translocating species occurs. In this case, NTRs would cause a breakdown of the barrier. The problem should occur already at low NTR concentrations and would worsen with time. Eventually, the gel would disintegrate. (**B**) A scenario where resealing behind the translocating species is slow. In this case, NTRs would transiently collapse the barrier. The problem would increase with the load of facilitated gel entry. (**C**) A scenario where the barrier reseals immediately behind a translocating species. In this case, the barrier would stay tight against inert material, even at the highest transport load.

MBP-mCherry with 1.5 μM of an IBB-MBP-mEGFP•scImpβ complex and allowed both species to enter the gel simultaneously. This NTR•cargo complex has a 2.4-fold higher mass and an 1.4-fold larger Stokes radius (R_S) than MBP-mCherry (Figure 3D), yet it entered the gel at least 100 times faster (Figures 2D and 3B, Table I). The acceleration of influx was specific for the scImpβ-bound cargo, because gel entry of the MBP-mCherry fusion, which lacked an import signal, was not enhanced in the presence of the importin (compare Figure 3A and B). Strikingly, we observed the same behaviour when the FG hydrogel was challenged with an even larger NTR•cargo complex (500 kDa, $R_S = 6.7$ nm) and a smaller inert permeation probe (mCherry, 27 kDa, $R_S = 2.4$ nm) (see Supplementary Figure S6). Thus, even large perforations formed by invading NTR•cargo complexes are not accessed by inert permeation probes. Instead, such lesions are short-lived and seal immediately behind the translocating species.

The assay should be very sensitive to even a low fraction of persisting perforations, because the scImpβ•cargo complex is considerably larger than the passive cargo and because a very

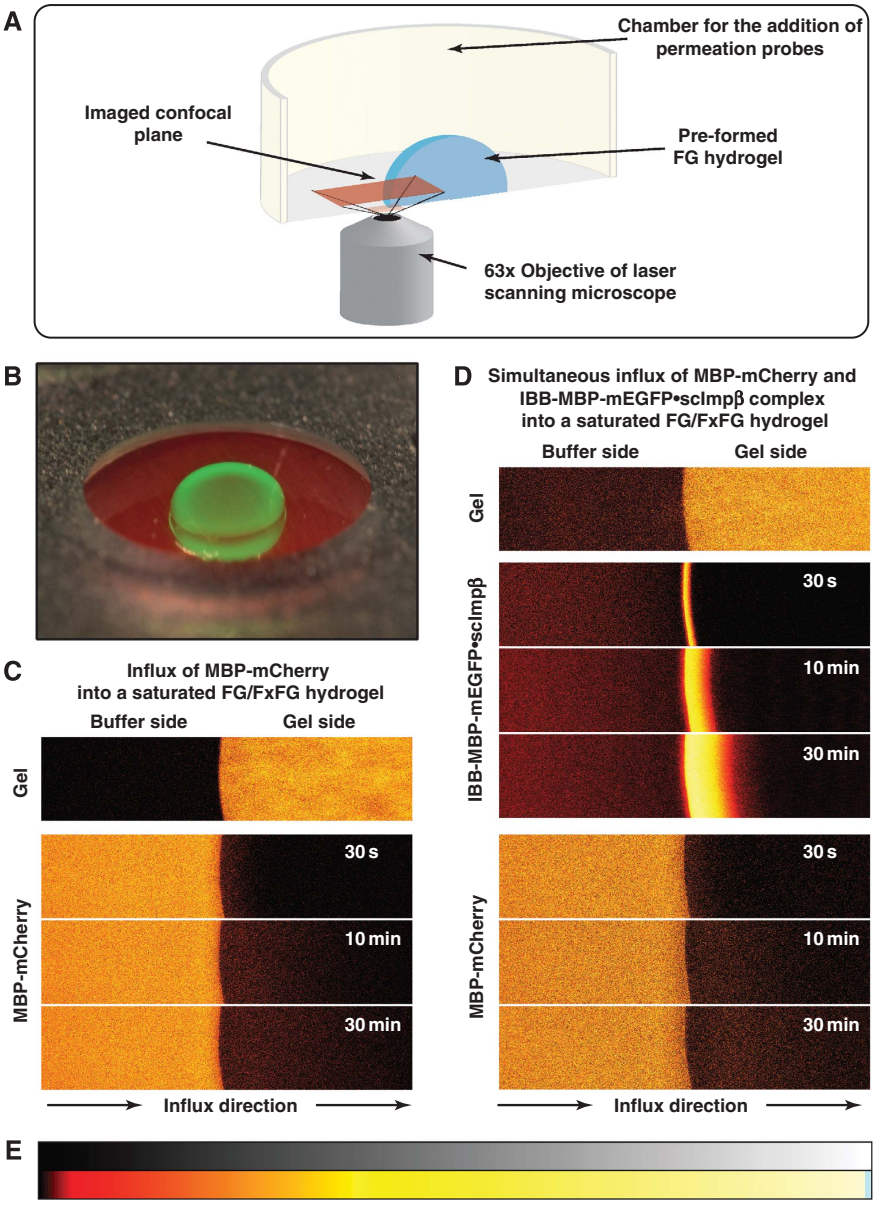

Figure 2 Experimental set-up for studying influx into an FG hydrogel. (**A**) Illustration of the experimental set-up. (**B**) A saturated FG/FxFG$^{Nsp1}_{2-601}$ hydrogel within the imaging chamber after completion of an influx experiment. Photographs were taken using a macro lens either under white light or UV illumination and overlaid. Note that the green NTR•cargo complex (IBB-MBP-mEGFP•scImpβ) entered the gel, whereas the red inert reference molecule (MBP-mCherry) stayed out. (**C**) Influx of MBP-mCherry alone into a saturated FG/FxFG$^{Nsp1}_{2-601}$ hydrogel followed by laser scanning confocal microscopy. Time elapsed after addition is indicated. Upper panels show the gel as detected by an incorporated Atto647N-labelled tracer molecule. Lower panels show 3 μM of MBP-mCherry added to the buffer side of the gel. The gel contained 200 mg/ml of FG/FxFG$^{Nsp1}_{2-601}$. For quantification see Figure 3 and Table I. For false-colour code, see panel E. (**D**) Experiment shows simultaneous influx of MBP-mCherry and IBB-MBP-mEGFP•scImpβ complex into the same batch of hydrogel as shown in panel C. Note that the rapid influx of the NTR•cargo complex did not detectably increase the entry of the non-receptor-bound inert reference molecule MBP-mCherry. For quantification, see Figure 3. (**E**) Look-up table used for translation of grey scale into false-colour images.

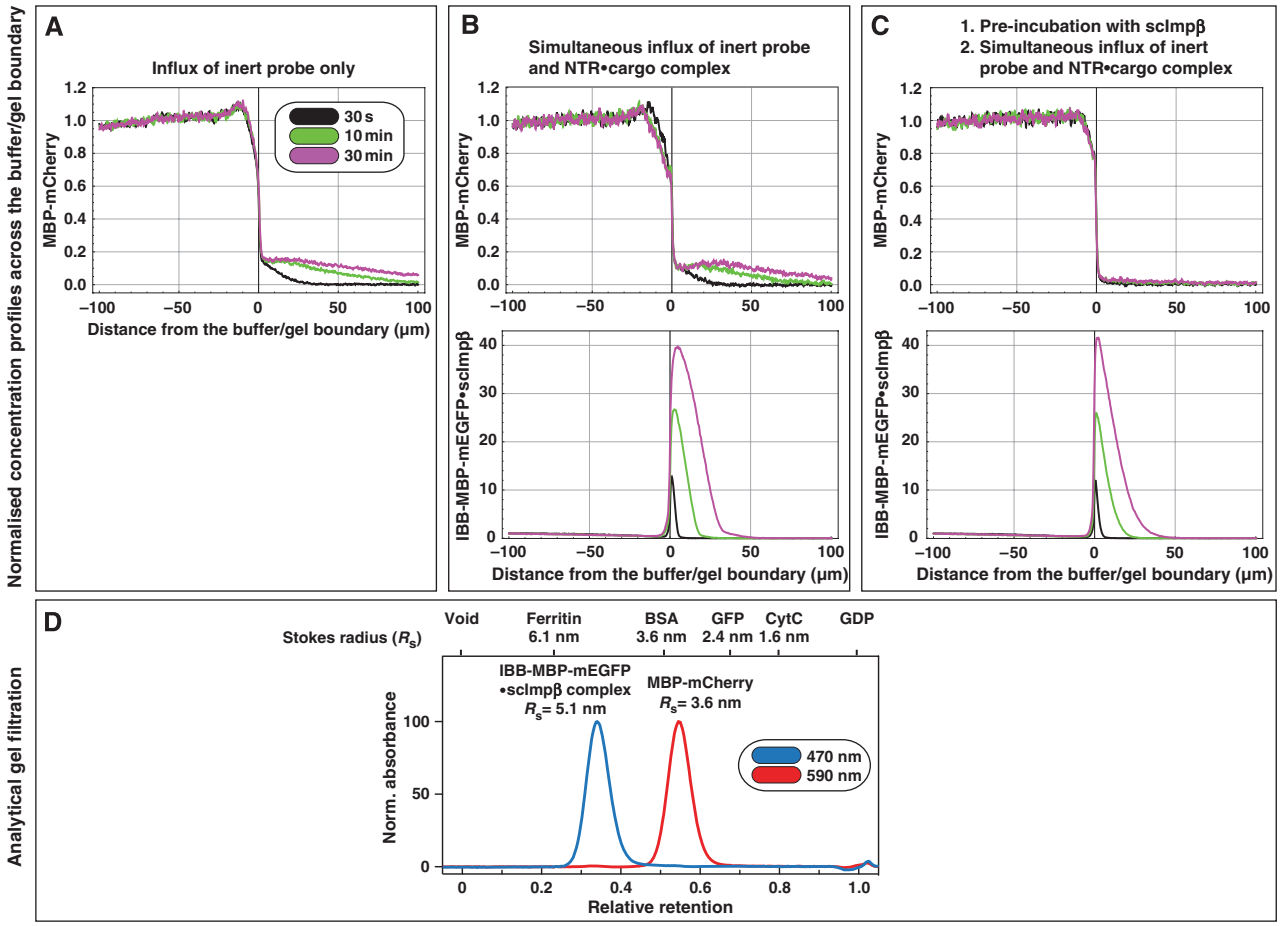

Figure 3 Pre-incubation of the FG/FxFG hydrogel with scImpβ tightens the barrier against passive influx. Panels A–C show concentration profiles of mobile species during their entry into a saturated FG/FxFG$^{Nsp1}_{2-601}$ hydrogel. The three time points (30 s, 10 min and 30 min) are colour-coded. For best comparison, the free concentration of the mobile species in buffer was scaled to 1. (**A**) Influx of MBP-mCherry alone. The comparison of the three time points indicates a slow, but still clearly detectable influx and a partition coefficient between gel and buffer of 0.18. (**B**) Simultaneous influx of 3 μM of MBP-mCherry and 1 μM of an IBB-MBP-mEGFP•scImpβ complex. The NTR•cargo complex entered the gel ≈100 times faster than the passive species. The presence of the NTR•cargo complex did not increase influx of the passive species as compared with panel A. (**C**) The influx experiment was performed as in panel B, the difference being that the FG hydrogel had been pre-incubated for 180 min with 10 μM of unlabelled, cargo-free scImpβ before the fluorescent mobile species was added. The pretreatment had only a minor effect on influx of the NTR•cargo complex (slight reduction in entry rate and intra-gel diffusion coefficient), indicating that this type of FG hydrogel is very robust against competition and can sustain a very high load of facilitated transport. However, the pretreatment had the striking effect of tightening the barrier against passive influx, and thus improving the performance of the barrier greatly. The labelled scImpβ•cargo complex now entered the gel at least 5000 times faster than the inert reference molecule MBP-mCherry. (**D**) Analytical gel filtration revealed a Stokes radius (R_S) of 3.6 nm for the above used inert reference molecule (MBP-mCherry) and 5.1 nm for the IBB-MBP-mEGFP•scImpβ complex.

large number of scImpβ•cargo complexes, namely ≈1 million per μm^2 per minute, had entered the gel (Figure 3). This number indicates that every point on the gel surface had been perforated on average more than 100 times per minute (for derivation see Materials and methods). The experiments therefore suggest that resealing behind a translocating species is efficient not only in intact NPCs but also when an FG hydrogel of very simple composition is used as a barrier.

NTRs even tighten the barrier against passive influx

We then performed a more drastic version of the experiment and pre-incubated the saturated FG/FxFG$^{Nsp1}_{2-601}$ hydrogel for 3 h with 10 μM of scImpβ. This concentration should mimic a physiological transport receptor concentration, which is in the range of 1 μM for individual receptors and ≈10 μM for the total NTR concentration (U Jäkle and D Görlich, unpublished results, 2001). During this pre-incubation, scImpβ accumulated inside the gel at a concentration of ≈0.5 mM (≈50 mg/ml; data not shown). Interestingly, this pre-load hardly diminished the subsequent influx of the fluorescent IBB-MBP-mEGFP•scImpβ complex (Figure 3C). This documents an enormous capacity of this FG hydrogel for facilitated translocation, comparable with that of authentic NPCs, which sustain a flux of ≈100 MDa per pore per second (Ribbeck and Görlich, 2001). The pre-incubation with scImpβ had, however, a marked effect on the inert permeation probe and reduced the influx of MBP-mCherry to virtually non-detectable levels, that is, at least 50-fold (Figure 3C, Table I). This effect was not only kinetic, but in fact the pre-incubation of the gel lowered the partition coefficient of the passive species between gel and buffer from 0.2 in an untreated gel to ⩽0.02, indicating that partitioning of MBP-mCherry into the gel became energetically even less favourable. For comparison, under the same conditions, the partition coefficient of the scImpβ•cargo complex (⩾100) was 5000-fold higher. The selectivity of

Table I Quantitation of influx of various mobile species into different types of FG hydrogels

Gel type	Mobile species	Pre-incubated with 10 μM of	Partition coefficient of mobile species between gel and buffer	Entry rate of mobile species into the barrier (nm/s)	Intra-gel diffusion constant of mobile species (10^{-12} m^2/s)	Passage time through an NPC (ms)[a]
Gel entry of NTR•cargo complexes						
FG/FxFG	IBB-MBP-mEGFP•scImpβ	—	⩾100	⩾3000	0.17	7
FG/FxFG	IBB-MBP-mEGFP•scImpβ	scImpβ	⩾100	⩾3000	0.12	10
GLFG	IBB-MBP-mEGFP•scImpβ	—	⩾400	⩾20 000	0.10	12
GLFG	IBB-MBP-mEGFP•scImpβ	scImpβ	⩾100	⩾4000	0.08	16
GLFG	IBB-MBP-mEGFP•scImpβ	hsImpβ$^{45\text{-}462}$	5	≈50	0.005	250
FG/FxFG/GLFG	IBB-MBP-mEGFP•scImpβ	—	⩾350	⩾15 000	0.24	5
FG/FxFG/GLFG	IBB-MBP-mEGFP•scImpβ	scImpβ	⩾400	12 000	0.30	4
Gel entry of inert molecules						
FG/FxFG	MBP-mCherry	—	0.16	40		
FG/FxFG	MBP-mCherry	scImpβ	0.02	0.6		
FG/FxFG	mCherry	—	0.42	180		
FG/FxFG	mCherry	IBB-MBP-mEGFP•scImpβ	<0.02	<1		

For details of parameter estimation see Frey and Görlich (2007).
[a]Estimation of passage time of mobile species through an NPC, whose 50 nm thick permeability barrier is filled with the specified FG hydrogel. For comparison, the passage time of Impβ•cargo complexes through authentic NPCs is in the order of 10 ms (Kubitscheck *et al*, 2005; Yang and Musser, 2006).

NPCs or of an FG hydrogel can be expressed as the ratio between the entry rates of a facilitated and a passive species. It is truly remarkable that a high load of facilitated transport even improved the selectivity and thus the performance of the FG hydrogel as a barrier.

NTRs tighten the barrier even towards GFP-sized passive probes

We then repeated the series of experiments with a smaller inert permeation probe, namely mCherry, which has a mass of 30 kDa and an R_S of 2.4 nm (Figure 4D). As expected, owing to its smaller size, mCherry alone entered the gel ≈10-fold faster (Figure 4A) than the MBP-mCherry fusion (Figure 3A). Consistent with the results from Figure 3 and with the behaviour of authentic NPCs (Mohr *et al*, 2009), the simultaneous addition of an IBB-MBP-mEGFP•scImpβ complex did not increase influx of the passive species. Even on the contrary, it changed the concentration profile of the passive species such that a dent complementary to the concentration profile of the NTR•cargo complex occurred (see 30 min time point in Figure 4B and compare with Figure 3B), indicating that the partition coefficient of the passive species between gel and buffer had been lowered by the presence of the transport receptor in this region of the gel.

In the third experiment of this set, we pre-incubated the gel not with an empty NTR as in Figure 3, but with an IBB-MBP-mEGFP•scImpβ complex. This made a difference in several ways: (1) the receptor species used for the pre-incubation was more bulky and it should therefore melt larger holes into the gel (Figure 4D), (2) it was applied in its substrate-bound conformation and (3) the pre-accumulated NTR•cargo complex could be directly visualised and quantified within the gel. It reached an intra-gel concentration of ≈0.4 mM, corresponding to ≈70 mg/ml (Figure 4C, lower panel).

This pre-incubation had the striking effect of suppressing the gel entry of mCherry to nearly non-detectable levels, that is, at least 100-fold (Figure 4C, Table I; see also Supplementary Figure S6). The residual entry rate into the gel of <1 nm/s translates to a first-order rate constant for nucleo-cytoplasmic equilibration in HeLa cell nuclei of $<5\times10^{-6}\,s^{-1}$. In comparison, a GFP-sized protein equilibrates in permeabilised cells with a rate constant of $2\times10^{-3}\,s^{-1}$ (see Mohr *et al*, 2009). It thus appears that *in vitro* assembled FG hydrogel can perform significantly better as a passive diffusion barrier than NPCs themselves. In other words, the design of the system is so robust that NPCs do not need to exploit the full potential of FG hydrogels in order to keep nuclear contents and the cytoplasm separated.

Pre-loading of the FG hydrogel with an NTR•cargo complex strongly suppressed passive influx of inert material, but did not preclude facilitated gel entry. Instead, the chase experiment shown in Supplementary Figure S1 clearly shows that, even after extensive pre-loading, NTR•cargo complexes could efficiently enter such a very tight FG/FxFG hydrogel. In contrast, if the gel was similarly pre-treated with an anti-FG repeat antibody, a strikingly different effect was observed (Supplementary Figure S3). Such a gel lost its competence to mediate a facilitated entry, but still allowed a similar rate of passive influx as an untreated gel. These results indicate that the observed increase in selectivity is specific for gels pre-treated with NTRs.

The GLFG domains from Nup49p and Nup57p can also form a highly selective hydrogel

So far, we tested only the FG/FxFG$^{Nsp1}_{2\text{-}601}$ repeat domain from Nsp1p for hydrogel formation and generation of a selective permeability barrier. Authentic NPCs, however, also contain another major class of FG repeats, namely GLFG repeats (Wente *et al*, 1992; Wimmer *et al*, 1992), in

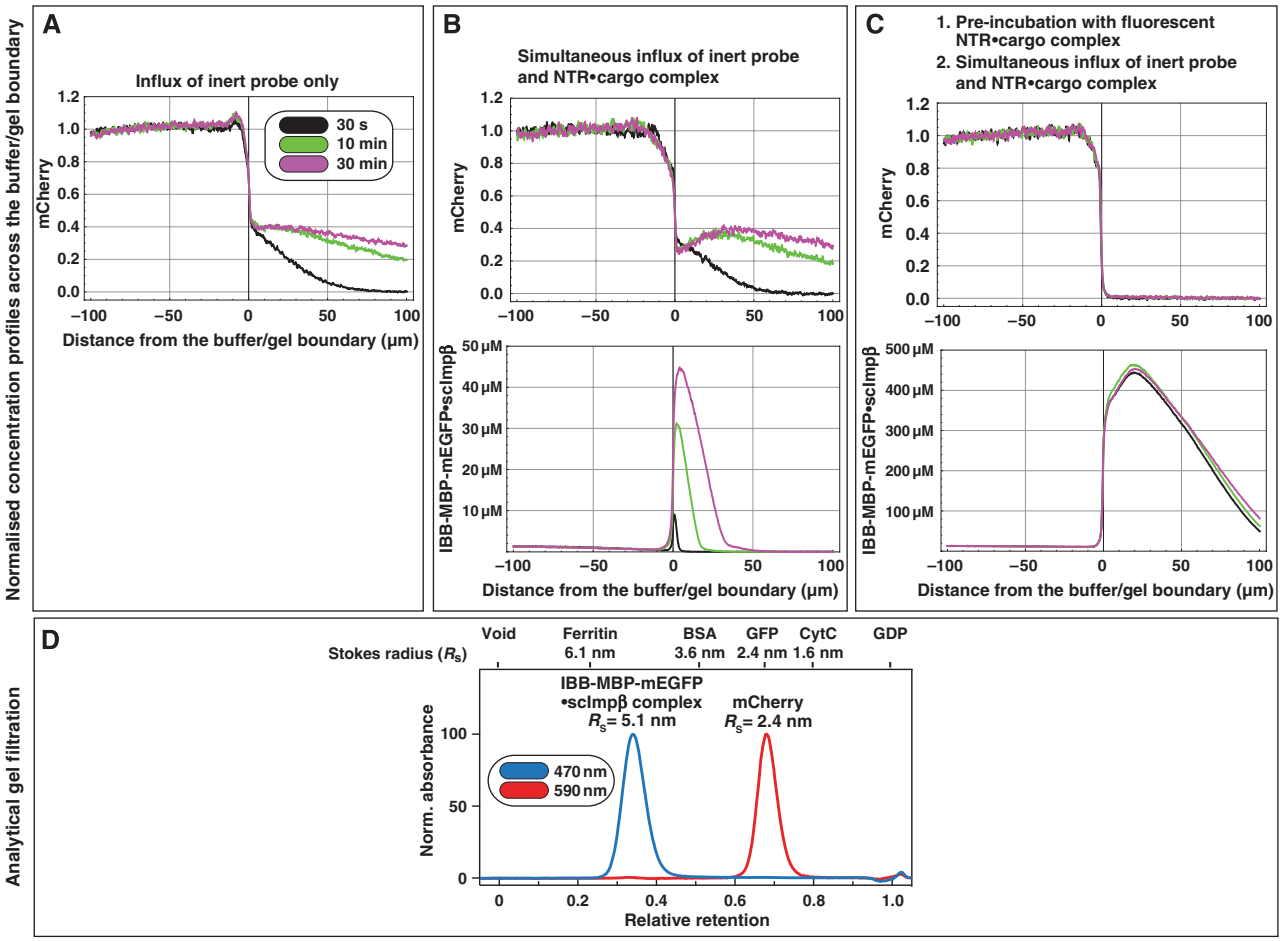

Figure 4 Facilitated translocation tightens the FG/FxFG hydrogel even against passive influx of GFP-sized objects. The influx experiment was carried out as in Figure 3, but two differences were implemented: First, we used a smaller inert reference molecule (mCherry, Stokes radius (R_S) = 2.4 nm) in order to enhance the sensitivity for small changes in passive permeability. Second, for pre-incubation, the 'empty' scImpβ was replaced by an IBB-MBP-mEGFP•scImpβ complex. The receptor used for the pre-incubation was therefore also detectable in the GFP channel. As expected from its smaller size, mCherry entered the untreated gel considerably faster than the MBP-mCherry fusion. The pre-incubation with the NTR•cargo complex diminished mCherry influx to very low levels. The pretreatment did, however, not abolish the NTR-mediated cargo entry (see Supplementary Figure 1).

which the NTR-binding hydrophobic clusters comprise a leucine and a phenylalanine sandwiched between two glycines. The repeat domain of Nsp1p becomes essential for the viability of *Saccharomyces cerevisiae* when certain other FG repeat domains are deleted (Strawn *et al*, 2004). Nevertheless, viable yeast strains that lack all FxFG repeat domains have been constructed. In contrast, yeast strains that lack all GLFG repeats are not viable (Strawn *et al*, 2004), indicating that *S. cerevisiae* relies more heavily on GLFG- than on FxFG-type repeats. It was therefore a crucial question as to whether GLFG repeat domains can also form a hydrogel, and if so, which permeability properties such gel would have.

To address these questions, we chose Nup49p (Wente *et al*, 1992; Wimmer *et al*, 1992) and Nup57p (Grandi *et al*, 1995) (1) because both proteins form a tight complex with Nsp1p (Grandi *et al*, 1995; Schlaich *et al*, 1997); (2) they are believed to be located near the central channel of the NPC, where the permeability barrier should have its most effective position; and (3) because strong genetic evidence suggests that their prototypical GLFG repeat domains are crucial for NPC function (Strawn *et al*, 2004). It should be noted that the repeat domains of Nup49p and Nup57p differ from the Nsp1p repeats not only in the different predominating hydrophobic clusters but also in that they lack charged residues in the intervening spacer sequences. For further analysis, we generated a fusion between the GLFG repeat domains of Nup49p and Nup57p, expressed the corresponding His-tagged fusion protein in *Escherichia coli* and purified it on a nickel chelate matrix.

Preparing a homogeneous FG hydrogel *in vitro* is a technically challenging task. It requires initially suppressing inter-repeat interactions so that a homogeneous and sufficiently concentrated solution of the FG repeat domain can be prepared before gel formation is initiated. We solved this problem by loading the protein in guanidinium chloride onto a C18 reverse-phase HPLC column and eluted the protein as a TFA salt with an aqueous acetonitrile gradient. From the protein-containing fractions, a lyophilisate was prepared, which readily dissolved to ≈200 mg/ml in water or 0.1% TFA, and subsequently formed a tough gel within a few hours of incubation. The resulting GLFG hydrogel had a similar appearance as the Nsp1p-derived FG/FxFG hydrogel (see Figure 2B) and was used after

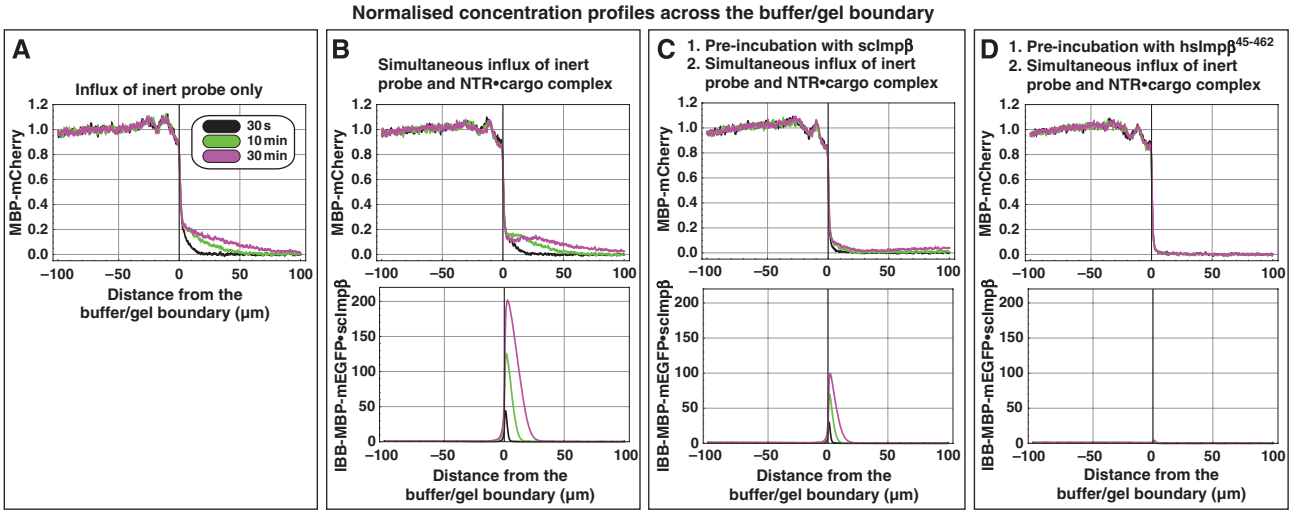

Figure 5 GLFG repeat domains also form a highly selective permeability barrier. Panels show influx of mobile species into a hydrogel made of 200 mg/ml of a fusion between the GLFG repeat domains of Nup49p and Nup57p. Quantification was carried out analogous to Figure 3. (**A**) Influx of 3 μM of MBP-mCherry alone. (**B**) Simultaneous influx of 3 μM of MBP-mCherry and 1 μM of IBB-MBP-mEGFP•scImpβ complex. (**C**) As panel B, however, the gel was pre-incubated for 180 min with 10 μM of scImpβ. This pre-incubation tightened the barrier against passive influx, but also diminished receptor-mediated cargo entry as well as intra-gel diffusion of the NTR•cargo complex, suggesting that the GLFG gel is more sensitive to competition by scImpβ than the FG/FxFG gel (see Figure 3C). (**D**) As panel B, however, the gel was pre-incubated with the dominant-negative human Impβ$^{45\text{-}462}$ fragment. This pre-incubation lead to a virtually complete block of passive influx and to a 100-fold reduction in receptor-mediated gel entry. Intra-gel movement of the scImpβ•cargo complex was essentially blocked (also see Supplementary Figure S4). The effect of the dominant-negative mutant on the GLFG gel was much stronger than on an FG/FxFG gel (see Supplementary Figure S4).

thorough equilibration in assay buffer for subsequent influx experiments.

Overall, the permeability properties of the GLFG gel appeared quite similar to the saturated FG/FxFG$^{Nsp1}_{2-601}$ gel that was characterised before (Figure 3 and Frey and Görlich, 2007): (1) The GLFG gel was a good barrier against influx of the MBP-mCherry fusion protein (Figure 5A, Table I), but also allowed a >100-fold faster influx of an NTR•cargo complex (Figure 5B). (2) Similar to previous experiments using an FG/FxFG gel (Frey and Görlich, 2007), influx of scImpβ into the GLFG gel was limited only by the diffusion to the gel. As the result of rapid influx and rate-limiting diffusion, a deep depletion zone of the transport receptor formed in front of the gel (data not shown, but see Frey and Görlich, 2007). (3) As was the case for the FG/FxFG gel (Figure 3C), an excess of transport receptor diminished the passive influx into the gel (Figure 5C). (4) Similar to the FG/FxFG gel (Frey and Görlich, 2007), the GLFG gel permitted facilitated entry not only of scImpβ but also of other NTRs. This was tested for the yeast importins Pse1p, Pdr6p and Yrb4p; the human importin transportin; and the yeast exportin Crm1p (Figure 6). In each case, the concentration profiles and entry rates were similar to scImpβ.

At closer inspection, however, notable differences between the different gel types became evident: compared with the FG/FxFG gel, the enrichment of scImpβ within the GLFG gel was 5-fold higher and intra-gel diffusion was ≈2-fold slower (compare Figures 3B and 5B and see Table I). Also, the influx of scImpβ•cargo complexes into the GLFG gel was more sensitive to competition by free scImpβ than was the entry into the FG/FxFG gel (compare Figures 3C and 5C). This competition not only diminished the influx of transport receptors but also their intra-gel movement (see Supplementary Figure S4 and Table I).

The largest difference, however, was in the response of the gels to the dominant-negative human Impβ$^{45\text{-}462}$ fragment, which is a strong inhibitor of facilitated NPC passage (Kutay *et al*, 1997b) and also inhibitory to passive passage of inert material, in particular if the inert objects are not too small (see Mohr *et al*, 2009). Pre-incubation with 10 μM of the dominant-negative mutant caused only about a three-fold reduction of scImpβ-mediated cargo influx into the FG/FxFG gel (Supplementary Figure S5). On the GLFG gel, however, it had a dramatic effect. It reduced the influx of the scImpβ•cargo complex into the GLFG gel by a factor of >100 (Figure 5 and Table I). The small amount of the NTR•cargo complex that had entered the gel remained close to the buffer/gel boundary and showed hardly any intra-gel movement, much as though the mutant had 'frozen' the gel (Supplementary Figure S4). The hsImpβ$^{45\text{-}462}$ fragment also diminished the passive influx of MBP-mCherry into the GLFG gel to nearly non-detectable levels (Figure 5D).

The assembly of FG repeat domains into a hydrogel is a multi-molecular reaction and should therefore show a high degree of cooperativity. Similar to a crystallisation process, one should expect that a critical protein concentration must be reached before the associates form. This critical concentration, however, is very different for the various FG repeat domains studied here. GLFG repeats show a high propensity to associate (Patel *et al*, 2007). This is evident from a phase separation of dilute GLFG solutions (e.g., 2 mg/ml) into a protein-rich and an aqueous phase (S Frey, unpublished results, 2007). In contrast, the FG/FxFG$^{Nsp1}_{2-601}$ domain stays fully soluble under the same conditions; it forms a gel only in sufficiently concentrated solutions (>7 to 10 mg/ml). This difference explains why bead-binding assays easily detected GLFG interactions, while inter-molecular interactions between the FG/FxFG$^{Nsp1}_{2-601}$ domain were less obvious (Patel

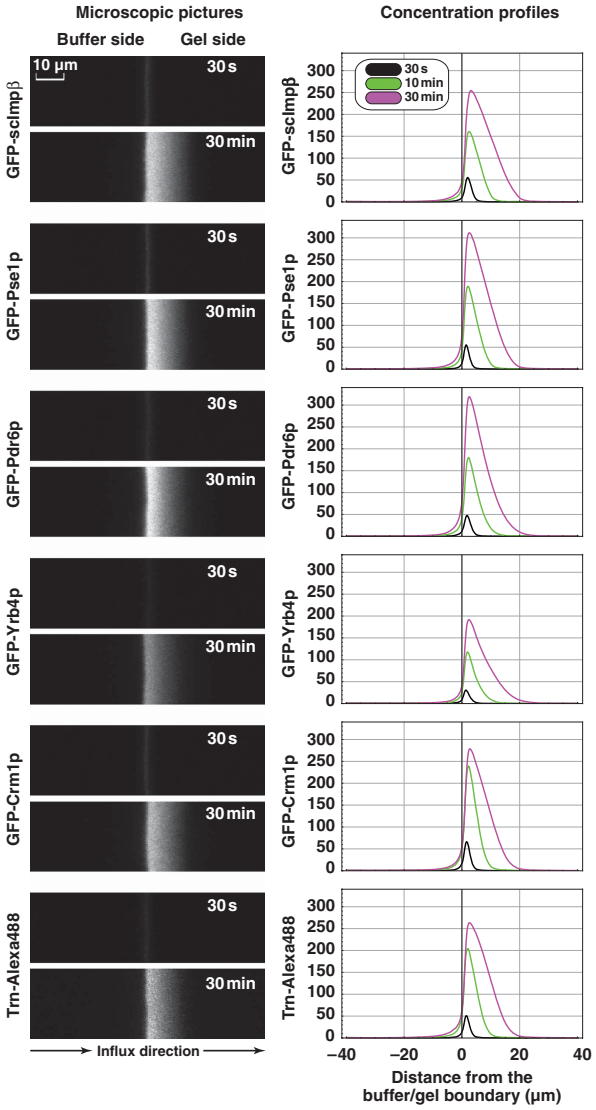

Figure 6 The GLFG hydrogel allows facilitated entry not only of scImpβ but also of other nuclear transport receptors (NTRs). The entry of the six indicated GFP-NTR fusions (1 µM concentration on buffer side) into a saturated GLFG hydrogel was studied. Left panels show microscopic images in the GFP channel at the 30-s and 30-min time points, all taken at identical settings. Right panels show quantifications. Note that all tested NTRs entered the gel rapidly and showed a similar intra-gel movement, corresponding to a passage time through an NPC of ≈10 to 20 ms.

et al, 2007). Apparently, it is mainly the high content of charged residues in the C-terminal part of the FG/FxFG$^{Nsp1}_{2-601}$ domain that attenuates self-association (C Ader, S Frey, W Mass, D Görlich and M Baldus, in preparation). The N-terminal part, FG/FxFG$^{Nsp1}_{2-601}$, in contrast, behaves very much like the GLFG repeats. Function-wise, however, these differences are probably not very dramatic, because the attachment to the rigid body of the NPC scaffold forces the FG repeat domains to a very high local concentration. And once formed, GLFG as well as FG/FxFG gels are kinetically stable, they do not dissolve in excess of buffer and show similar permeabilities.

Mixed FG/FxFG/GLFG hydrogels

Authentic NPCs contain various types of FG repeats. This posed the question whether mixed hydrogels made up of FG, FxFG and GLFG repeats would show a qualitatively different behaviour than either an FG/FxFG or a GLFG gel. To test this, we generated a fusion protein comprising the GLFG repeat domain from Nup57p, the FG/FxFG repeat domain from Nsp1p and the GLFG repeat domain from Nup49p. The fusion protein was expressed, purified and jellified at a saturating concentration as described for the pure GLFG repeat domain.

The resulting mixed FG/FxFG/GLFG hydrogel performed again very well as a selective barrier. It suppressed the passive entry of inert material and allowed rapid influx of scImpβ•cargo complexes (Figure 7). The rate of facilitated entry matched the influx into the GLFG gel and even exceeded the influx into an FG/FxFG gel (see Figure 8 for a direct comparison). At the same time, intra-gel diffusion of the NTRs appeared more than two times faster than within a pure GLFG gel and slightly faster than within the FG/FxFG gel. These quantitative differences point to different on and off rates of the various repeat motifs for NTR binding and for engaging in inter-repeat contacts. They suggest that certain NTRs traverse heterotypic FG•GLFG or FxFG•GLFG contacts more easily than homotypic GLFG contacts.

Compared with the pure GLFG gel, facilitated entry into the mixed hydrogel was more tolerant towards competition by an excess of transport receptors. Apparently, this reflects the fact that the mixed hydrogel also contains low-affinity NTR-binding sites that become saturated only at high receptor concentrations.

Combined, these data are consistent with the view that, owing to the higher diversity of hydrophobic patches and intervening spacer sequences, the mixed FG hydrogel is more robust and performs slightly better in the uptake of NTR•cargo complexes, in particular at higher transport loads. Overall, however, it was surprising to see how similar the permeability properties of FG/FxFG, GLFG and mixed FG/FxFG/GLFG hydrogels are. Although we do not yet know the atomic details of the intra-gel interactions, our data already suggest that functionally equivalent inter-repeat contacts can be created with various sequences.

Efflux from an FG hydrogel

The fact that NTRs dissolve with a very high partition coefficient within FG hydrogels poses the question if they can exit such a gel again. In addressing this question, we faced the difficulty that efflux of the NTR only yields a very weak signal outside the gel. In addition, it is hard to judge whether an observed NTR signal in the buffer is specific and originates from NTR molecules that previously resided in the gel. To overcome these problems, we used phenyl–sepharose beads, which bind NTRs very tightly (Ribbeck and Görlich, 2002). They served not only as local sinks for NTRs in the buffer but also to detect the direction of the NTR source. Therefore, after thorough removal of any free complex, we placed the beads in front of an FG hydrogel that had been preloaded with scImpβ•cargo complex. Over time, the beads attracted a strong scImpβ•cargo signal that showed a strikingly crescent-shaped distribution, with the regions of strongest staining pointing towards the gel (Figure 9A). This distribution indicates that the accumulated material indeed originated from the gel and was not just a remnant from the initial pre-incubation. Consistent with the assumption that the NTR molecules left the gel and diffused through buffer to

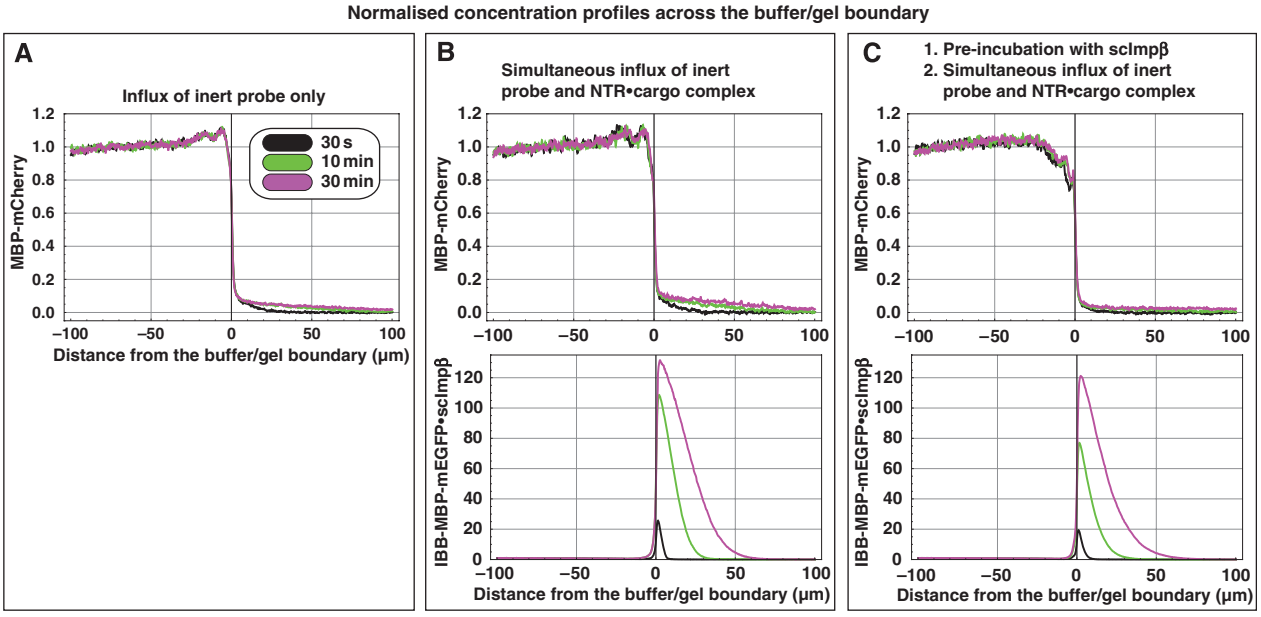

Figure 7 Behaviour of a mixed FG/FxFG/GLFG hydrogel. A triple fusion comprising the FG repeat domains of the central Nsp1p•Nup49p•Nup57p complex was used to prepare a saturated FG hydrogel. Panels show quantification of influx into such gel, using the same probes and experimental conditions as in Figure 3A–C.

the beads, no direct contact between beads and gel was required for the effect.

We then repeated the experiment without a phenyl–sepharose sink (Figure 9B). As expected, also in this set-up, a weak efflux of the NTR•cargo complex from the gel into the buffer was observed (compare 1- and 180-min time points in Figure 9B). This efflux was clearly enhanced when GTP-Gsp1p (the yeast Ran orthologue) was added to the buffer side. Here, Ran probably acts through two mechanisms: it dissociates the cargo from Impβ (Rexach and Blobel, 1995; Görlich *et al*, 1996b) and weakens the interaction of Impβ with FG repeats (Harel *et al*, 2003; Walther *et al*, 2003). The first mechanism is evident from the fact that more cargo than scImpβ was released from the gel (Fig 9B). The second mechanism is evident because Gsp1p also increased the efflux of scImpβ. Within cells, Impα•Impβ and IBB•Impβ complexes arrest at NPCs, until nuclear RanGTP terminates the translocation and releases cargo and Impα into the nucleus (Moore and Blobel, 1993; Görlich *et al*, 1996b). The observation that this reaction can be reproduced with an *in vitro* assembled FG hydrogel lends further support to the assumption that the permeability barrier of NPCs is indeed made up of such a gel.

Discussion

Models of NPC function

NPCs have a dual function. On the one hand, they must suppress intermixing of nuclear and cytoplasmic contents, while on the other they have to allow for efficient receptor-mediated biosynthetic transport, which supplies nuclei with proteins and the cytoplasm with translation components such as ribosomes. The mechanism of NPC function has been the key question since the early days of the nuclear transport field and many attempts have been made to explain the selectivity of nuclear pores.

Early models suggested, for example, that NPCs function like an iris diaphragm that is closed in the resting state, but opens for each transiting signal-bearing cargo (see e.g., Akey, 1992). Such purely 'mechanical' model appears unrealistic from today's perspective. However, it is useful to illustrate the principal problems of a 'general gating' mechanism: The barrier would break down whenever the gate is open, and because facilitated transport load is so high that NPCs must even transport many cargoes in parallel (Ribbeck and Görlich, 2001), such mechanism cannot explain how NPCs keep nuclear and cytoplasmic contents separated from each other. Nevertheless, it is indeed possible that large-scale rigid-body movements of the entire NPC widen the central channel and facilitate passage of exceptionally large cargoes, such as ribosomal subunits. However, also such a widened pore has to be sealed against non-selective passage of inert material by a *bona fide* permeability barrier.

Meanwhile, it is accepted that FG repeat domains not only bind NTRs but also build the permeability barrier (Frey and Görlich, 2007; Patel *et al*, 2007). How these FG repeats form the barrier has been cast into different models (Macara, 2001; Ribbeck and Görlich, 2001; Rout *et al*, 2003). The 'virtual gate model' assumes that entropic exclusion by Brownian motion of the extended FG repeat domains is sufficient to explain the suppression of passive fluxes through NPCs and that NTRs overcome this 'entropic barrier' by binding the repeats (Rout *et al*, 2003). Although peripheral, non-interacting FG repeat domains might indeed enlarge the target area of NPCs and 'feed' NTRs into the actual permeability barrier, this model could so far not explain the characteristic size selectivity of NPCs.

Numerous observations speak in favour of the FG hydrogel or selective phase model (Ribbeck and Görlich, 2001; Frey and Görlich, 2007). It differs from the virtual gate model foremost by the assumption that FG repeat domains interact

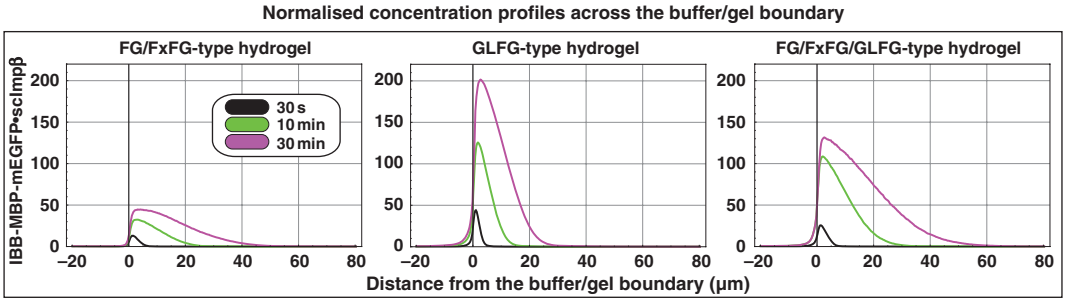

Figure 8 Comparison of scImpβ-mediated facilitated entry into different types of FG hydrogels. To allow a direct comparison between FG/FxFG, GLFG, and mixed hydrogels, influx of IBB-MBP-mEGFP•scImpβ complex into these gels was measured at identical settings and quantifications were plotted to identical scales. The FG/FxFG gel (left panel) showed the weakest enrichment of the NTR•cargo complex and fast intra-gel diffusion. The GLFG gel (middle panel) was characterised by a much stronger enrichment and slower intra-gel diffusion of the mobile species. The mixed FG/FxFG/GLFG gel (right panel) showed an intermediate enrichment of the transport receptor and yet fast intra-gel diffusion. It appeared to be the most efficient gel in terms of absorbing the transport receptor.

with each other, thereby forming a hydrogel. The gel-forming interactions comprise an essential hydrophobic component (Frey *et al*, 2006) as well as hydrophilic contacts (C Ader, S Frey, W Mass, D Görlich and M Baldus, in preparation), indirect contacts mediated by NTRs (this study) and possibly also entanglement between different FG repeat domains. The mesh size of this gel, corresponding roughly to the length of one repeat unit (typical 3–6 nm), determines the size limit for unhindered passage of inert material. This fits nicely the observation that GFP-sized objects (diameter $\approx$5 nm) are already significantly delayed in their NPC passage, whereas smaller ones, such as aprotinin (diameter of 3 nm) experience little resistance (see Mohr *et al*, 2009).

We have shown that the FG/FxFG repeat domain from Nsp1p (Frey and Görlich, 2007) as well as the GLFG repeat domains from Nup49p and Nup57p (this study) not only form hydrogels but also that these hydrogels behave like highly selective barriers. They exclude inert macromolecules, while similarly sized macromolecules recruited to an NTR can enter the gel up to four orders of magnitude faster. It should be noted that binding to FG motifs is necessary but not sufficient for facilitated entry into the FG hydrogel. For example, antibodies directed against FG motifs only bind to the surface of the gel and fail to penetrate into the gel (Supplementary Figure S2), probably because they are unable to dissociate inter-repeat contacts. The behaviour of NTRs is therefore highly specific.

Importantly, NTR-mediated influx rates into *in vitro* assembled, saturated FG hydrogels are similar to passage rates through authentic NPCs (Table I; Ribbeck and Görlich, 2001; Ribbeck and Görlich, 2002). Similarly, the intra-gel diffusion coefficients of NTR•cargo complexes allowed a remarkably accurate estimation of NPC passage times and vice versa (Table I; Kubitscheck *et al*, 2005; Yang and Musser, 2006; Frey and Görlich, 2007). In addition, we have shown that the hydrogel system also reproduces the exit of NTR•cargo complexes and that exit of an scImpβ•cargo complex from the gel is stimulated by RanGTP (Figure 9), which recapitulates results obtained with intact NPCs.

NTRs even tighten the barrier

The most stringent requirement to the permeability barrier is to stay tight against passive entry even when facilitated influx occurs. Here, we provide proof of concept that FG hydrogels fully fulfil this requirement. Similar to authentic NPCs (Newmeyer *et al*, 1986; Ribbeck and Görlich, 2001; Naim *et al*, 2006; Mohr *et al*, 2009), FG/FxFG, GLFG and mixed hydrogels can sustain a tremendous facilitated influx of NTRs and NTR•cargo complexes (Table I, Figures 3–5 and 7). Nevertheless, these gels remain tight barriers for inert molecules that are not NTR-bound. This suggests that the permeability barrier seals tightly around a translocating species and that the holes, which need to be melted into the barrier for accommodating translocating material, are very short lived. Amazingly, the barrier even tightens with increasing translocation load. This applies to *bona fide* NPCs (Mohr *et al*, 2009) as well as to the *in vitro* reconstituted permeability barrier (this study).

There are several straightforward explanations for this effect. The first relates to volume exclusion. scImpβ reaches high concentrations inside the gel, namely an estimated 0.5 mM (50 mg/ml) after 180 min of pre-incubation with 10 μM of scImpβ. It should then occupy 10–20% of the available volume of the gel, thereby posing additional obstacles for inert species entering the gel and forcing the structures formed by the FG domains to shrink to smaller effective mesh sizes. Furthermore, as the NTRs bind the FG motifs, this process will increase the total number of contacts within the gel and 'subdivide' meshes into smaller ones. In other words, NTRs not only become enclosed by the barrier but also participate in barrier function; they hinder inert material from traversing NPCs and they lower the FG repeat concentration required for proper barrier function.

The selectivity factor of NPCs

NTRs accelerate NPC passage of a bound cargo compared with free inert macromolecules of the same size. The magnitude of the effect depends on the size of the transported species. A protein as small as aprotinin or a z-domain traverses NPCs already as rapidly as a transport receptor (Mohr *et al*, 2009); such rapid passage can therefore not be further accelerated. A significant acceleration can only be observed for larger objects. The acceleration factor is around 10–100 for GFP-sized objects and can be >10 000 in the case of the 120-kDa tetrameric RedStar protein (Frey and Görlich, 2007; this study).

The magnitude of the effect, however, is not constant for a given inert molecule, but it increases with facilitated transport load. mCherry, for example, entered 'virgin' gels 100 times more slowly than scImpβ•cargo complexes. Preloading

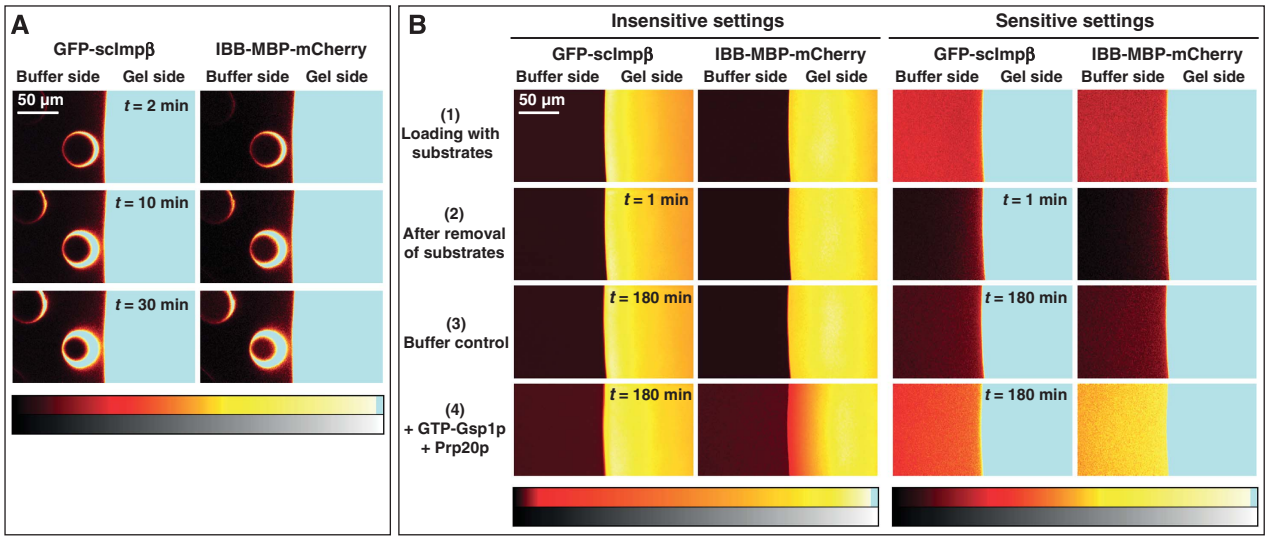

Figure 9 Entry of NTR•cargo complexes into an FG hydrogel is reversible. (**A**) A saturated FG/FxFG$^{Nsp1}_{2–601}$ hydrogel was preloaded overnight with an NTR•cargo complex (1 μM of GFP-scImpβ•IBB-MBP-mCherry in the buffer). The free complex was removed by several buffer changes and phenyl–sepharose beads were placed in front of the gel. Then, confocal scans detecting cargo and receptor were started. The beads served as a trap for scImpβ and strongly accumulated NTR and cargo over time. The accumulated signal was strongest on the side that faced the gel, identifying the hydrogel as the source of the NTR•cargo complex. Bar diagrams translate false colour look-up tables into grey scale. (**B**) An FG hydrogel was loaded with 1 μM of NTR•cargo complex as in panel A. The first scan (1) shows the loading of the gel. (2) A preloaded gel immediately after removing the free NTR•cargo complex by three buffer changes. (3) A preloaded gel after 3 h incubation with buffer and (4) after incubation with 4 μM of GTP-Gsp1p (*S. cerevisiae* Ran). Gsp1p increased the efflux of the cargo and of scImpβ from the gel. Two different scan settings of the experiment are shown, optimised to visualise either low or high protein concentrations.

of the barrier with NTRs improved this to a factor of 10 000 by suppressing the passive influx, while leaving facilitated entry (at least into the FG/FxFG gel) largely unaffected. The selectivity factor of 10 000 leads to the better performance of the defined FG hydrogels than that of authentic NPCs in permeabilised cells. This observation emphasises that the FG hydrogel-based permeability barrier is an extremely robust and stress-tolerant system and it suggests that cells hardly ever need to exhaust the full potential of this sorting system.

A recent study (Jovanovic-Talisman *et al*, 2009) describes artificial nanopores filled with FG repeats from Nsp1p. These reproduced some features of NPCs, but even when NTRs were used to improve the barrier, these nanopores only reached a selectivity factor of 3–5. One possible explanation for this 10- to 1000-fold poorer performance compared with authentic NPCs and with the FG hydrogels is that the coupling density of the repeat domains within the nanopores was too low and did not reach the saturation limit.

The response of authentic NPCs to the dominant-negative human Impβ$^{45-462}$ mutant is reproduced by FG hydrogels

A very interesting parallel between authentic NPCs and the FG hydrogels is the effect of the dominant-negative human Impβ$^{45-462}$ fragment. Already at low concentrations it blocks all tested NTR-mediated pathways through NPCs (Kutay *et al*, 1997b) and also inhibits passive NPC passage of GFP-sized or larger inert objects (Mohr *et al*, 2009). The hsImpβ$^{45-462}$ mutant is deficient in Ran binding and it was initially assumed that its great inhibitory potential is due to the fact that RanGTP cannot release the mutant from high-affinity binding sites on the nuclear side of the NPC (Kutay *et al*, 1997b). This is, however, only a part of the explanation. The mutant oligomerises (see Mohr *et al*, 2009) and it is probably the multiplicity of binding sites in the oligomer that allows the mutant to bind that avidly to certain FG repeats.

The mutant, however, does not block all FG repeats. Instead, NLS•Impα•Impβ complexes could still dock to NPCs that had been clogged by the mutant (Kutay *et al*, 1997b). Similarly, we observed that the mutant had only a minor impact on the FG/FxFG$^{Nsp1}_{2–601}$ gel, but severely inhibited the entry of NTR•cargo complexes and inert objects into the GLFG gel. Interestingly, the mutant also markedly impaired diffusion within the GLFG gel and, thus, locked the gel in a non-dynamic, 'frozen' state. This illustrates nicely that an affinity for FG gel repeats is not sufficient for effectively crossing the barrier. Instead, the strength and quality of the interactions must be well balanced. In view of the discussion regarding models of NPC function, the parallel observations of the mutant's effects on authentic NPCs and *in vitro* assembled FG hydrogels make another point, that is, they strongly suggest that facilitated NPC passage and NTR-mediated entry into an FG hydrogel represent essentially the same process.

Materials and methods

E. coli expression vectors

Plasmids used in this study are summarised in Table II. The backbone of the indicated expression vectors was typically derived from pQE80 (Qiagen, Hilden, Germany). Exceptions are labelled explicitly. Plasmids allow for recombinant expression of indicated proteins in *E. coli*. DNA sequences coding for recombinant proteins are supplied as Supplementary data. Complete plasmid sequences are available on request.

Expression, purification and labelling of proteins

Expression and purification of the following proteins were carried out as previously described: Alexa488-labelled transportin (Ribbeck and Görlich, 2001) and hsImpβ$^{45-462}$-His$_6$ (Kutay *et al*, 1997b).

Table II *Escherichia coli* expression vectors

Name	Protein name	Expressed protein	Reference
pSF345	Nsp1FG/FxFG	His_{10}-TEV-$Nsp1p^{2-601}$-Cys	Frey *et al* (2006)
pSF847	Nup57GLFG-Nup49GLFG	His_{10}-TEV-$Nup57p^{1-233}$-$Nup49p^{1-246}$-Cys	This study
pSF776	Nup57GLFG-Nsp1FG/FxFG-Nup49GLFG	His_{10}-TEV-$Nup57p^{1-233}$-$Nsp1p^{2-601}$-$Nup49p^{1-246}$-Cys	This study
pSF851	IBB-MBP-mEGFP	His_{14}-TEV-IBB-MBP-mEGFP	This study
pSF844	MBP-mCherry	His_{14}-TEV-MBP-mCherry	This study; Shaner *et al* (2004)
pSF846	mCherry	His_{14}-TEV-mCherry	This study
pSF856	IBB-MBP-mCherry	His_{14}-TEV-IBB-MBP-mCherry	This study
pSF881	IBB-ZsGreen	His_{14}-TEV-IBB-ZsGreen	This study; Matz *et al* (1999)
pQE30-scImpβ	Importin β (Kap95p)	scImpβ-His_6	Görlich *et al* (1996b)
pSF582	GFP-Pdr6p (Kap122p)	His_{10}-GFP-TEV-Pdr6p	Frey and Görlich (2007)
pSF586	GFP-Yrb4p (Kap123p)	His_{10}-GFP-TEV-Yrb4p	Frey and Görlich (2007)
pSF587	GFP-importin β (Kap95p)	His_{10}-GFP-TEV-scImpβ	Frey and Görlich (2007)
pSF588	GFP-Pse1p (Kap121p)	His_{10}-GFP-TEV-Pse1p	Frey and Görlich (2007)
pSF879	GFP-Crm1p	His_{10}-GFP-TEV-Crm1p	This study
pQE60-hsTrn1	Human transportin1	His_6-transportin1	Izaurralde *et al* (1997)
pQE60-hsImpβ$^{45-462}$	hsImpβ$^{45-462}$	hsImpβ$^{45-462}$-His_6	Kutay *et al* (1997b)

His_6/His_{10}/His_{14}, histidine tag; IBB, importin β-binding domain (corresponding to amino acids 2-63 of *Saccharomyces cerevisiae* Srp1p); TEV, TEV protease recognition site.

For expression of diffusion substrates, *E. coli* strain BLR was transformed with the respective plasmid and grown at 25°C to $OD_{600} = 1–2$ in TB medium supplemented with 50 μg/ml kanamycin. Protein expression was induced with 0.3 mM of IPTG and cells were further allowed to grow at 18°C overnight. A total of 1 mM of PMSF (phenylmethylsulphonyl fluoride) and 5 mM of EDTA were added to the culture. After centrifugation and resuspension of the cell pellet in HS buffer (50 mM Tris–HCl (pH 8.0), 2 M NaCl, 5 mM $MgCl_2$, 0.5 mM EDTA, 1 mM imidazole, 10 mM DTT), the cells were disrupted by sonification and the lysate was cleared by centrifugation at 37 000 r.p.m. for 60 min. Cleared lysates were applied to nickel–sepharose equilibrated with HS buffer. After washing off unbound proteins with HS buffer followed by buffer A (44 mM Tris–HCl (pH 7.5), 290 mM NaCl, 4.4 mM $MgCl_2$, 0.44 mM EDTA, 2 mM DTT), proteins were eluted with buffer A supplemented with 300 mM of imidazole. The His-tag was cut off with TEV protease (1:50 enzyme to substrate ratio) at room temperature. Cut proteins were further purified by gel filtration on a Superdex 200 16/60 column (Pharmacia) equilibrated with buffer A followed by a second passage over nickel–sepharose. Purified proteins were supplemented with 1/10 volume of 2.5 M sucrose, concentrated to 100 μM and frozen in liquid nitrogen.

Expression of His_{10}-GFP-tagged NTRs and scImpβ-His_6 was performed similarly. Briefly, cells were grown in 2YT medium supplemented with 2% glycerol, 30 mM of K_2HPO_4 and appropriate antibiotics. Expression was induced with 0.5 mM of IPTG and allowed to proceed for 3–4 h at 25°C. Cell lysis and washing steps were carried out in buffer C (50 mM Tris–HCl (pH 7.5), 200 mM NaCl, 1 mM EDTA, 2 mM DTT) supplemented with 1 mM of imidazole. Proteins eluted from the nickel–sepharose were directly purified by gel filtration equilibrated with buffer C.

Nucleoporin FG repeat domains were expressed and purified essentially as previously described for FG/$FxFG^{Nsp1}_{2-601}$ (Frey *et al*, 2006). Briefly, repeat domains were expressed in *E. coli* and purified on nickel–sepharose under denaturing conditions. If necessary, eluted proteins were subjected to covalent chromatography on a thiopyridine-activated, SH-reactive matrix. To obtain fluorescently labelled repeat domains, the C-terminal cysteine was reacted with Atto647N maleimide. All repeat domains were purified by reverse-phase HPLC, eluted with increasing concentrations of acetonitrile in 0.15% TFA and lyophilised.

For purity of recombinant proteins, see Supplementary Figure S7.

Analytical gel filtration

Each pair of NTR•cargo complex and inert diffusion substrate was mixed with plasmid DNA and GDP as markers for the void volume (V_0) or total volume (V_{tot}) of the column, respectively, and analysed by gel filtration on a Superdex 200 10/30 column (Pharmacia) equilibrated with buffer B (20 mM Tris–HCl (pH 7.5), 130 mM NaCl, 2 mM $MgCl_2$, 0.2 mM EDTA) supplemented with 2 mM DTT. The column was calibrated with a mixture of plasmid DNA, Ferritin, BSA, GFP, cytochrome *c* and GDP. Relative retention (R_r) values were determined from the absolute retention volumes (V_{abs}) according to the formula: $R_r = (V_{abs} - V_0)/(V_{tot} - V_0)$.

Preparation of FG repeat hydrogels

Lyophilised repeat domains (TFA salt) were dissolved at a concentration of 200 mg protein per ml in 0.2% TFA. A volume of 0.7–1.0 μl drops were spotted onto uncoated 18-well microslides (ibidi, Munich, Germany) and allowed to complete gelation for 12–24 h. GLFG-containing repeat domains jellified already at low pH. Gel formation of the Nsp1 FG/FxFG repeat domain was initiated by adding 200 mM of Tris base. All gels were complemented by 0.3 μM of the respective Atto647N-labelled repeat domain. Before performing influx experiments, gels were equilibrated for 24 h in a large excess of buffer B (20 mM Tris–HCl (pH 7.5), 130 mM NaCl, 2 mM $MgCl_2$, 0.2 mM EDTA).

Microscopy

Gel entry of fluorescent substrate molecules was assayed using an SP5 confocal laser scanning microscope equipped with a 63× glycerol immersion objective (Leica, Bensheim, Germany). Briefly, the buffer/gel boundary was positioned at the centre of the observable area and the focal plane set to 5 μm above the surface of the slide. A total of 31 frames (1024 × 512 pixels) were recorded in intervals of 60 s in appropriate channels, using the 633-nm laser line to monitor the position of the gel and either the 458-nm laser line (for GFP, ZsGreen or Alexa488 fluorescence) or the 561-nm laser line (for mCherry fluorescence). Fluorescent substrates (in buffer B) were added after recording of the first frame. mCherry and MBP-mCherry were used at 3 μM concentration, the monomeric scImpβ•cargo complex was pre-formed from 1.3 μM IBB-MBP-mEGFP and 1.3 μM scImpβ, if not explicitly noted differently. The IBB-ZsGreen•scImpβ complex was pre-formed using an 1.3-fold excess of scImpβ over theoretically available IBB signals and purified from free scImpβ by gel filtration. For pre-incubations, the complex was used at 2.5 μM final concentration (tetrameric complex) in the buffer reservoir. Fluorescent NTRs were used at a concentration of 1 μM.

Antibodies

Antibodies against the FG/FxFG repeat domain of Nsp1p (amino acids 2-601) were raised in rabbits and affinity purified using the immobilised antigen. For fluorescent labelling, the antibody was reacted with DyLight488 NHS ester (Thermo Scientific) in PBS. The final preparation contained ~1.4 molecules of dye per IgG molecule.

Estimation of the number of NTR entry events per μm^2 gel surface

During the 30 min of the experiment (Figure 3), the scImpβ•cargo complex spread ≈50 μm deep into the gel, reaching an average concentration of ≈150 μM. This corresponds to an influx of 45 million molecules per μm^2. Given that an scImpβ•cargo complex projects to 80 nm^2, this indicates that every point on the gel surface had been perforated more than 3000 times within 30 min or 100 times per min.

Numerical evaluation of fluxes into the gels

This was essentially performed as previously described (Frey and Görlich, 2007).

Supplementary data

Supplementary data are available at *The EMBO Journal* Online (http://www.embojournal.org).

Acknowledgements

We thank T Güttler for critical reading, H Behr and J Schünemann for excellent technical help. We also thank the Max-Planck-Gesellschaft for financial support.

Conflict of interest

The authors declare that they have no conflict of interest.

References

Adam SA (2001) The nuclear pore complex. *Genome Biol* **2:** REVIEWS0007

Akey CW (1992) The nuclear pore complex: a macromolecular transport machine. In *Nuclear Trafficking*, Feldherr, CM (ed), pp 31–70. New York: Academic Press

Bayliss R, Leung SW, Baker RP, Quimby BB, Corbett AH, Stewart M (2002) Structural basis for the interaction between NTF2 and nucleoporin FxFG repeats. *EMBO J* **21:** 2843–2853

Bayliss R, Littlewood T, Stewart M (2000) Structural basis for the interaction between FxFG nucleoporin repeats and importin-beta in nuclear trafficking. *Cell* **102:** 99–108

Bayliss R, Ribbeck K, Akin D, Kent HM, Feldherr CM, Görlich D, Stewart M (1999) Interaction between NTF2 and xFxFG-containing nucleoporins is required to mediate nuclear import of RanGDP. *J Mol Biol* **293:** 579–593

Bednenko J, Cingolani G, Gerace L (2003) Importin beta contains a COOH-terminal nucleoporin binding region important for nuclear transport. *J Cell Biol* **162:** 391–401

Chi NC, Adam EJ, Adam SA (1995) Sequence and characterization of cytoplasmic nuclear protein import factor p97. *J Cell Biol* **130:** 265–274

D'Angelo MA, Hetzer MW (2008) Structure, dynamics and function of nuclear pore complexes. *Trends Cell Biol* **18:** 456–466

Denning DP, Patel SS, Uversky V, Fink AL, Rexach M (2003) Disorder in the nuclear pore complex: the FG repeat regions of nucleoporins are natively unfolded. *Proc Natl Acad Sci USA* **100:** 2450–2455

Denning DP, Rexach MF (2007) Rapid evolution exposes the boundaries of domain structure and function in natively unfolded FG nucleoporins. *Mol Cell Proteomics* **6:** 272–282

Englmeier L, Olivo JC, Mattaj IW (1999) Receptor-mediated substrate translocation through the nuclear pore complex without nucleotide triphosphate hydrolysis. *Curr Biol* **9:** 30–41

Fornerod M, Ohno M, Yoshida M, Mattaj IW (1997) Crm1 is an export receptor for leucine rich nuclear export signals. *Cell* **90:** 1051–1060

Frey S, Görlich D (2007) A saturated FG-repeat hydrogel can reproduce the permeability properties of nuclear pore complexes. *Cell* **130:** 512–523

Frey S, Richter RP, Görlich D (2006) FG-rich repeats of nuclear pore proteins form a three-dimensional meshwork with hydrogel-like properties. *Science* **314:** 815–817

Görlich D, Henklein P, Laskey R, Hartmann E (1996a) A 41 amino acid motif in importin alpha confers binding to importin beta and hence transit into the nucleus. *EMBO J* **15:** 1810–1817

Görlich D, Kostka S, Kraft R, Dingwall C, Laskey RA, Hartmann E, Prehn S (1995) Two different subunits of importin cooperate to recognize nuclear localization signals and bind them to the nuclear envelope. *Curr Biol* **5:** 383–392

Görlich D, Kutay U (1999) Transport between the cell nucleus and the cytoplasm. *Annu Rev Cell Dev Biol* **15:** 607–660

Görlich D, Pante N, Kutay U, Aebi U, Bischoff FR (1996b) Identification of different roles for RanGDP and RanGTP in nuclear protein import. *EMBO J* **15:** 5584–5594

Grandi P, Schlaich N, Tekotte H, Hurt EC (1995) Functional interaction of Nic96p with a core nucleoporin complex consisting of Nsp1p, Nup49p and a novel protein Nup57p. *EMBO J* **14:** 76–87

Harel A, Chan RC, Lachish-Zalait A, Zimmerman E, Elbaum M, Forbes DJ (2003) Importin beta negatively regulates nuclear membrane fusion and nuclear pore complex assembly. *Mol Biol Cell* **14:** 4387–4396

Hurt EC (1988) A novel nucleoskeletal-like protein located at the nuclear periphery is required for the life cycle of *Saccharomyces cerevisiae*. *EMBO J* **7:** 4323–4434

Iovine MK, Watkins JL, Wente SR (1995) The GLFG repetitive region of the nucleoporin Nup116p interacts with Kap95p, an essential yeast nuclear import factor. *J Cell Biol* **131:** 1699–1713

Isgro T, Schulten K (2005) Binding dynamics of isolated nucleoporin repeat regions to importin-β. *Structure* **13:** 1869–1879

Izaurralde E, Kutay U, von Kobbe C, Mattaj IW, Görlich D (1997) The asymmetric distribution of the constituents of the Ran system is essential for transport into and out of the nucleus. *EMBO J* **16:** 6535–6547

Jovanovic-Talisman T, Tetenbaum-Novatt J, McKenney AS, Zilman A, Peters R, Rout MP, Chait BT (2009) Artificial nanopores that mimic the transport selectivity of the nuclear pore complex. *Nature* **457:** 1023–1027

Kubitscheck U, Grunwald D, Hoekstra A, Rohleder D, Kues T, Siebrasse JP, Peters R (2005) Nuclear transport of single molecules: dwell times at the nuclear pore complex. *J Cell Biol* **168:** 233–243

Kutay U, Bischoff FR, Kostka S, Kraft R, Görlich D (1997a) Export of importin alpha from the nucleus is mediated by a specific nuclear transport factor. *Cell* **90:** 1061–1071

Kutay U, Izaurralde E, Bischoff FR, Mattaj IW, Görlich D (1997b) Dominant-negative mutants of importin-beta block multiple pathways of import and export through the nuclear pore complex. *EMBO J* **16:** 1153–1163

Macara IG (2001) Transport into and out of the nucleus. *Microbiol Mol Biol Rev* **65:** 570–594

Mattaj IW, Englmeier L (1998) Nucleocytoplasmic transport: the soluble phase. *Annu Rev Biochem* **67:** 265–306

Matz MV, Fradkov AF, Labas YA, Savitsky AP, Zaraisky AG, Markelov ML, Lukyanov SA (1999) Fluorescent proteins from nonbioluminescent Anthozoa species. *Nat Biotechnol* **17:** 969–973

Mohr D, Frey S, Fischer T, Güttler T, Görlich D (2009) Characterisation of the passive permeability barrier of nuclear pore complexes. *EMBO J* (advance online publication, 13 August 2009)

Moore M, Blobel G (1993) The GTP-binding protein Ran/TC4 is required for protein import into the nucleus. *Nature* **365:** 661–663

Morrison J, Yang JC, Stewart M, Neuhaus D (2003) Solution NMR study of the interaction between NTF2 and nucleoporin FxFG repeats. *J Mol Biol* **333:** 587–603

Naim B, Brumfeld V, Kapon R, Kiss V, Nevo R, Reich Z (2006) Passive and facilitated transport in nuclear pore complexes is largely uncoupled. *J Biol Chem* **282:** 3881–3888

Newmeyer DD, Finlay DR, Forbes DJ (1986) *In vitro* transport of a fluorescent nuclear protein and exclusion of non-nuclear proteins. *J Cell Biol* **103:** 2091–2102

Patel SS, Belmont BJ, Sante JM, Rexach MF (2007) Natively unfolded nucleoporins gate protein diffusion across the nuclear pore complex. *Cell* **129:** 83–96

Pemberton LF, Paschal BM (2005) Mechanisms of receptor-mediated nuclear import and nuclear export. *Traffic* **6:** 187–198

Rexach M, Blobel G (1995) Protein import into nuclei: association and dissociation reactions involving transport substrate, transport factors, and nucleoporins. *Cell* **83:** 683–692

Ribbeck K, Görlich D (2001) Kinetic analysis of translocation through nuclear pore complexes. *EMBO J* **20:** 1320–1330

Ribbeck K, Görlich D (2002) The permeability barrier of nuclear pore complexes appears to operate via hydrophobic exclusion. *EMBO J* **21:** 2664–2671

Ribbeck K, Kutay U, Paraskeva E, Görlich D (1999) The translocation of transportin–cargo complexes through nuclear pores is independent of both Ran and energy. *Curr Biol* **9:** 47–50

Rout MP, Aitchison JD (2001) The nuclear pore complex as a transport machine. *J Biol Chem* **276:** 16593–16596

Rout MP, Aitchison JD, Magnasco MO, Chait BT (2003) Virtual gating and nuclear transport: the hole picture. *Trends Cell Biol* **13:** 622–628

Rout MP, Aitchison JD, Suprapto A, Hjertaas K, Zhao Y, Chait BT (2000) The yeast nuclear pore complex: composition, architecture, and transport mechanism. *J Cell Biol* **148:** 635–651

Schlaich NL, Haner M, Lustig A, Aebi U, Hurt EC (1997) *In vitro* reconstitution of a heterotrimeric nucleoporin complex consisting of recombinant Nsp1p, Nup49p, and Nup57p. *Mol Biol Cell* **8:** 33–46

Schwoebel ED, Talcott B, Cushman I, Moore MS (1998) Ran-dependent signal-mediated nuclear import does not require GTP hydrolysis by Ran. *J Biol Chem* **273:** 35170–35175

Shaner N, Campbell R, Steinbach P, Giepmans B, Palmer A, Tsien R (2004) Improved monomeric red, orange and yellow fluorescent proteins derived from *Discosoma* sp. red fluorescent protein. *Nat Biotechnol* **22:** 1567–1572

Stade K, Ford CS, Guthrie C, Weis K (1997) Exportin 1 (Crm1p) is an essential nuclear export factor. *Cell* **90:** 1041–1050

Strawn LA, Shen T, Shulga N, Goldfarb DS, Wente SR (2004) Minimal nuclear pore complexes define FG repeat domains essential for transport. *Nat Cell Biol* **6:** 197–206

Tran EJ, Wente SR (2006) Dynamic nuclear pore complexes: life on the edge. *Cell* **125:** 1041–1053

Walther TC, Askjaer P, Gentzel M, Habermann A, Griffiths G, Wilm M, Mattaj IW, Hetzer M (2003) RanGTP mediates nuclear pore complex assembly. *Nature* **424:** 689–694

Weis K, Ryder U, Lamond AI (1996) The conserved amino-terminal domain of hSRP1 alpha is essential for nuclear protein import. *EMBO J* **15:** 1818–1825

Wente SR, Rout MP, Blobel G (1992) A new family of yeast nuclear pore complex proteins. *J Cell Biol* **119:** 705–723

Wimmer C, Doye V, Grandi P, Nehrbass U, Hurt EC (1992) A new subclass of nucleoporins that functionally interact with nuclear pore protein Nsp1. *EMBO J* **11:** 5051–5061

Yang W, Musser SM (2006) Nuclear import time and transport efficiency depend on importin beta concentration. *J Cell Biol* **174:** 951–961